Computer Networks and Communications
https://ojs.wiserpub.com/index.php/CNC

Article

UAV base-station design method and optimization for urban environment communication with 5G cellular network

Valencia Lala[1,2], Wang Desheng[1], Joao Andre Ndombasi Diakusala[3], Feno Heriniaina Rabevohitra[4], Nour Mohammad Murad[5], Glauco Filho Fontgalland[6], Raul Sanchez Galan[7], Glauco Fontgalland[6] and Blaise Ravelo[8]

[1] Huazhong University of Science and Technology, Electronic Information and Communications, Wuhan, Hubei, China
[2] Institut Supérieur de Technologie D'Antsiranana (IST-D), BP 509, Antsiranana 201, Madagascar
[3] Nanjing University of Information Science & Technology (NUIST), School of Artificial Intelligence (School of Future Technology), Nanjing, China 210044
[4] Studio MG, Antananarivo 101, Madagascar
[5] PIMENT, Network and Telecom Lab, Institut Universitaire de Technologie, University of La Réunion, Saint Pierre 97410, France
[6] Brenton School of Engineering University of Mount Union, Alliance, OH 44601 USA
[7] 4i Intelligent Insights, Tecnoincubadora Marie Curie, PCT Cartuja, 41092 Sevilla, Spain
[8] Nanjing University of Information Science & Technology (NUIST), School of Electronic & Information Engineering, Nanjing, China 210044
E-mail: lalasoavalencia@gmail.com, dswang@hust.edu.cn, njadnissi@gmail.com, fenoheriniaina@studio.mg, nour.murad@univ-reunion.fr, glauco.filho@ee.ufcg.edu.br, r.sanchez@4i.ai, fontgalland@gmail.com, blaise.ravelo@yahoo.fr
*Corresponding author: blaise.ravelo@yahoo.fr

Received: 29 April 2025; **Revised:** 30 June 2025; **Accepted:** 17 July 2025

Abstract: During unexpected or temporary events, base transceiver stations (BTSs), also known as base stations (BSs), may be unable to fully meet the flexibility and resilience requirements of upcoming cellular networks. A promising solution to this issue is to serve the cellular networks with low-altitude unmanned aerial vehicle base stations (UAV-BSs), which can assist terrestrial stations in increasing networks' capacity and coverage. This paper proposes a network planning method for the fast deployment of fifth-generation (5G) cellular networks using a metaheuristic algorithm. This approach aims to determine the minimum number of UAV-BSs that can cover an area the size of a stadium while considering cell capacity, coverage constraints, the system's spectral efficiency, and the battery life of the UAVs being utilized. We have formulated an optimization problem approach to capture the practical aspects and satisfy the above conditions simultaneously. We have detailed the implementation of a metaheuristic algorithm based on particle swarm optimization (PSO) that finds optimal locations for the UAV-BSs that satisfy all the stadium constraints among various subareas with different user densities. This approach was compared to a genetic algorithm (GA) using the same simulation parameters during performance evaluation. The simulation results indicate that the proposed approach effectively finds the minimum number of UAV-BSs and their 3-D placement so that all users are served based on their traffic requirements. The results also indicate that the quality-of-service (QoS) targets desired for the network are reached in each scenario.

Keywords: Unmanned aerial vehicles (UAV), UAV deployment planning, fast-deployment 5G network, UAV base station (UAV-BS), Particle Swarm Optimization (PSO), UAV system design method, Genetic algorithm (GA), Optimization technique.

DOI: https://doi.org/10.37256/cnc.3220257142

1. INTRODUCTION

The evolution of our modern lifestyle depends fundamentally on mobile communication [1-2] via the Internet of Things (IoTs) [3] and smart objects [4-5]. Emerging wireless solutions have been deployed in information communication technology (ICT). Different generations of ICT have been developed to provide a better quality of service (QoS) [1-5] to users. Recent surveys on the reliability of the 5G network [6-13] have shown that, in terms of the success of modern society, a reliable connection is no longer a privilege but a requirement for communication, surveillance, and security [14-15]. Based on this constant need for connectivity, the deployment of Unmanned Aerial Vehicles (UAVs) [16-18] for temporary or emergency flying wireless network connections has attracted more attention to the research community [19-26]. However, relevant modeling is required to reduce the cost of deployment and guarantee the QoS while effectively operating UAVs as mobile base transceiver stations (BTSs), also known as base stations (BSs). The following subsection introduces a brief overview of modeling based on UAV or drone communication. UAVs, frequently known as drones, are flying platforms including to provide cellular network coverage, create device-to-device relay networks, offer surveillance and monitoring, and delivery of medical supplies. The use of UAVs has been rapidly growing in the last few years due to their autonomy, mobility, flexibility, adaptive altitude, and wide-ranging application areas [17-19]. In wireless communication, UAVs can offer solutions in terms of portability, reliability, and cost-effectiveness if they are correctly deployed and operated. One example of such is the use of UAVs as aerial base stations (UAV-BSs). Based on the available proximity network as well as the need, UAV-BSs can work either independently or simultaneously with existing terrestrial wireless networks to provide, extend, or enhance the coverage of the cellular network during temporary events. One of the main advantages of using an aerial base station is the possibility and flexibility of changing its position when the line-of-sight (LoS) link [27-31] between the base station and the user is hindered. Thus, relocating the UAV base station is enough to reduce the non-LoS (NLoS) link and provide full and stable coverage to the targeted area. In addition, each drone has a mobile capability that makes it easy to deploy during emergencies, such as during or after a natural disaster, during which a failure on ground communication infrastructure has been affected or is non-existent [16,17,27,28,29,30], to provide additional support to all devices requiring wireless connections. Despite the promising applications of UAV-based communication systems, regulation is one of the major limiting factors in the deployment of said systems, as they differ according to their categories [19] and based on each country's internal regulations. Placements of a single UAV-BS have been rigorously studied [20–22] and should be done in such a way that covers as many users as possible while using the least amount of transmitted power possible or following some rules based on the requirements of ground users. However, these works do not cover the cases of multiple aerial deployments if we needed to cover a broader range of ground users, which would necessitate the general coordination of the UAVs. Furthermore, for better efficiency, one should consider only deploying the least number of UAVs required based on the area that needs to be covered. Moreover, although the placement of multiple UAV-BSs has recently attracted more interest from both practitioners and the scientific community [23–26], the identified challenges can be narrowed down to five main issues: energy availability, mobility and path planning, placement of nodes, security and privacy issues, and the quality of service being provided. The overall goal of this research is to develop an efficient and quick simulation method for the deployment of 5G cellular network UAV-BS. To reach the expected technical goal, we:

- Introduce the desired model for the system,
- Followed by the optimization problem based on the predefined constraints, and,
- Elaborate the algorithm formulation.

The contributions of this paper are:

- To understand the design steps of cellular network planning with UAVs,
- To provide a simulation approach for the particle swarm optimization (PSO) algorithm and genetic algorithm (GA) for multiple UAV-BSs deployment and,
- To find the relevant method to determine the minimum needed UAV-BSs in order to effectively server the targeted ground users and to minimize interference when servicing ground users and avoid competition between the UAV-BSs.

The rest of this paper is organized as follows:

- Section 2 introduces the design description of the UAV-BS cellular network system deployment and describes the dimensioning of the UAV-BS cellular network system.
- Section 3 elaborates on the optimization techniques and methodology of the UAV-BS cellular network system based on the PSO algorithm and the GA.
- Section 4 presents the optimization cell planning method based on the PSO algorithm and the GA.
- Section 5 introduces and provides a thorough description of the simulation process.

- Section 6 discusses the outcome of the simulation results for deploying the UAV-BS cellular network system during the day. The QoS performance is also discussed.
- Section 7 focuses on presenting simulation results and QoS performances from the different case studies considered for the deployment of the UAV-BS cellular network system.
- The last section is devoted to the discussion, conclusion, and future work.

2. DESCRIPTION OF THE DEPLOYMENT DESIGN OF THE UAV-BS cellular network SYSTEM

2.1 Problem statement of the urban environment scenario

A surface area the size of a football field must temporarily be covered by the 5G network through the use of the UAV cellular network system model. Figure 1 shows the scenario of an event organized in a stadium that has a BTS nearby.

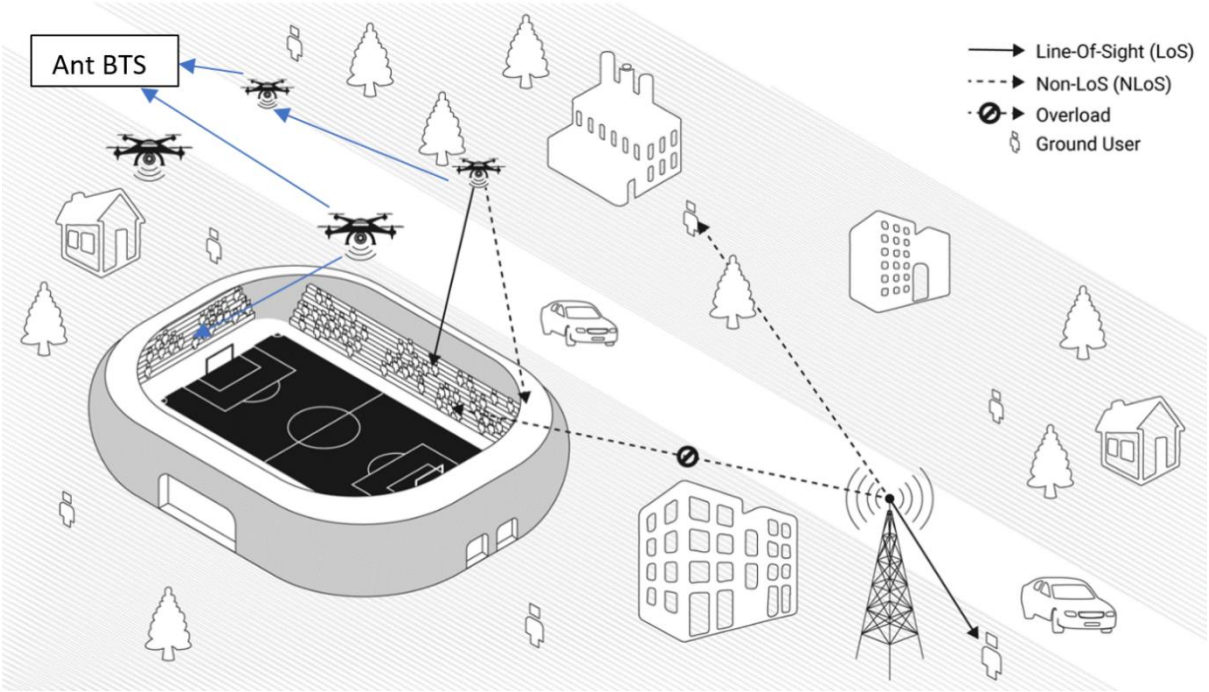

Figure 1 3-D perspective view representing the system model of the case study.

However, when people gather in the stadium, the network is not able to serve all the devices, thus the need for the rapid deployment of a UAV-BS cellular network system. The surface of the stadium, including the open-air stands, needs to be covered by the network. We assume the total number of users to serve will be 1,000, most of whom will be seated while others are performing on the field. The objective of this research is to coordinate the UAV-BS and find the minimum number needed in order to effectively serve all wireless mobile devices within our defined area and locate their respective optimal 3-D locations. Mobility is one of the essential features of the aerial BS and helps manage its deployment based on the users' locations. When the users move, the UAV-BS may have to relocate accordingly in order to serve them better. The following subsections further elaborate upon the geometrical 3-D configuration associated with the UAV-BS cellular network system model.

2.2 Efficient 3-D positioning of UAV base station

The 3-D positioning enables the placement of each drone unit within the space. It acts as a geometrical 3-D problem and can be considered a cartesian system, as shown in Figure 2.

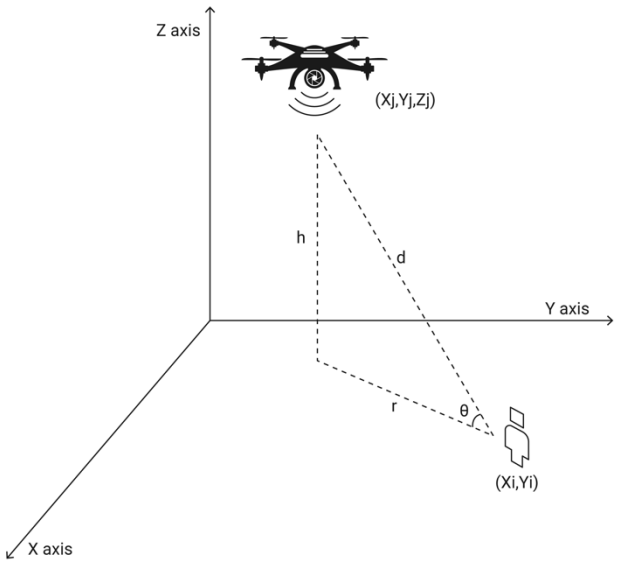

Figure 2 Illustration of 3-D coordinate cartesian system.

The main criteria of positioning are the drones acting as cellular BSs are scattered from each other, before the placement of the UAV in the horizontal space (x_j, y_j), we also need to determine their altitude (h_j) and considering a fixed transmission power, the area covered by a BTS is fixed unless the antenna is relocated. Relocation is a tedious task for BS and is one of the main advantages of using UAV-BS. The coverage of UAV-BS is relative to its flying altitude, latitude, and longitude. Thus, the exact coverage limit is known once the drone is in position. In contrast to base terrestrial station (BTS), the mobility of the UAV-BS allows for its relocation to a different position where the network coverage demand is high. Therefore, we need to find optimal placements (latitude, longitude, and altitude) at which the UAV-BSs should be located to ensure maximum network coverage for the targeted area. As the altitude of the device can vary over time, a change of transmission power is not essential to change the coverage areas, as up to a certain degree, this can be achieved by either increasing or decreasing the altitude of the UAV-BSs.

2.3 Flying time cycle and management

Events can take place at any time of the day or night and can last for hours, days, weeks, or even months. For the proposed system to be efficient and effective, the UAV's battery life is crucial and must be accounted for during the network planning. Selection of the drone is another important element as drones from different categories may have different capabilities in terms of flying time. However, energy consumption is not limited to maintaining the device in the air, but also plays a part in communication. The below initial assessment focuses on managing the UAV's battery lifetime while ensuring constant converge from the UAV-BS and finding the total number of the UAV-BSs needed to deploy in order to cover the defined area. In Table I, we provide a description of the notations and parameters used in this study. Let's consider a stadium packed with 1,000 ground users during the day and 60% of this amount at night.

Table I. List of notations for the initial dimensioning

Notation	Description
BW	Channel bandwidth in Hz
a	Average spectral efficiency of the system in bps/Hz
R^{dl}	Users target data rate in the downlink
N_{uBS}	Maximum number of users served by each UAV-BS
N_U^x	Total number of users in the stadium at x time
N_{BS}^x	Total number of UAV-BSs needed to be deployed
N_{BS}^{Day}	Total number of UAV-BSs needed to be deployed during the daytime
N_{BS}^{Night}	Total number of UAV-BSs needed to be deployed during the nighttime

In this scenario, N_{BS}^{Day} UAVs will be deployed during the day, and replaced by N_{BS}^{Night} UAVs at night. This establishes a cycle in which the UAVs that are used during the day can be recharged at night and their usage can resume the next day.

2.4 Capacity provisioning

Like standard BTSs, aerial BSs have a maximum number of users that can be served simultaneously, which we denote as N_{uBS}. We assume that the downlink (DL) data rate is generally more significant than the uplink (UL) data rate value. In terms of capacity provisioning, the DL is defined as the limiting link. The N_{uBS} can then be formulated as:

$$N_{uBS} = \left\lfloor \frac{BW\ \alpha}{R^{dl}} \right\rfloor \tag{1}$$

in which $\lfloor \cdot \rfloor$ represents the floor function, BW defines the capacity of the UAV-BS and R^{dl} is the target data rate that users aim to achieve in DL. To discover the number of BSs needed to satisfy the denoted downlink user data rate, we can use the following equation:

$$N_{BS}^{x} = \left\lceil \frac{N_{U}^{x}}{N_{uBS}} \right\rceil \tag{2}$$

With $\lceil \cdot \rceil$ represents the ceiling function, N_{U}^{x} is the total number of users in the stadium and x is a variable that is relative to the UAV-BS deploying time which can either be during the day or at night. From here, a good optimization technique is needed to ensure the performance of the UAV-BS cellular network system.

3. METHODOLOGY OF THE UAV-BS CELLULAR NETWORK SYSTEM OPTIMIZATION

Before we address the optimization process, we must properly describe the UAV-BS system problem as well as constraints to both capacity and coverage.

3.1 Description of the UAV-BS system optimization problem

The optimization problem aims to find an optimal location for the UAV-BS that satisfies the capacity and coverage constraints. This location can be analytically formulated based on a mathematical model. Thus, we must first elaborate on the notations for the present study with their descriptions in Table II.

Table II. List of notations for the optimization problem

Notation	Description
N_s	Total number of subareas
$\varepsilon_{j,s}$	The parameter that measures the presence of UAV-BS j in the subarea s
$a_{j,s}$	Intersection zone between the area covered by a UAV-BS j and the subarea s
A_j	Total area covered by a UAV-BS j
ξ	The least percentage of area desired to be covered by the UAV-BSs
D_s	User density in a subarea s
A_s	Surface of a subarea s
$E\left\{\frac{1}{\alpha_i}\right\}$	The expected value for a spectral efficiency i
γ_{ij}	SINR of a user i served by UAV-BS j
γ_{th}	The minimum SINR level required for each user
τ	The minimum percentage of users desired to be covered by the UAV-BSs
P_r^{DL} , P_r^{UL}	Power received in DL and UL
P_t^{UL} , P_t^{UL}	Power transmitted in DL and UL
N	Noise power
L_{dB}	Path loss of the channel in dB
β_i	Binary variable that denotes the state of a user i
ρ_i	Vector that contains the state of each UAV-BS

3.2 Description of capacity constraints

We divided the complete area that needs to be served into subareas N_s. The following parameter is defined to measure the presence of UAV-BS j in subarea s:

$$\varepsilon_{j,s} = \frac{a_{j,s}}{A_j} \tag{3}$$

in which:

- $j = 1,...,N_{BS}^{x}$ and s=1,…,N_s
- $a_{j,s}$ is the intersection zone between the area covered by the UAV-BS j and subarea s
- A_j is the total area covered by a UAV-BS j

We assume that the parameter $0 \le \varepsilon_{j,s} \le 1$ while respecting the following conditions:

- if the coverage of the UAV-BS j is totally included in subarea s, then $\varepsilon_{j,s} = 1$
- if it is partially contained in subarea s, then $\varepsilon_{j,s} < 1$
- if the UAV-BS j coverage and subarea s are not joined, then $\varepsilon_{j,s} = 0$

Hence, to serve all users in a given subarea s, the inequality in the following equation must be satisfied:

$$\sum_{j=1}^{N_{BS}^{x}} N_{uBS}\varepsilon_{j,s} \ge \xi A_s D_s \tag{4}$$

with s=1,…,N_s and where ξ is the minimum percentage of the area desired to be covered by UAV-BSs. D_s is the user density function in subarea s and A_s is the surface of subarea s. To ensure that the average spectral efficiency of the system is higher or equal to α (the value used in the initial dimensioning), the following condition must be considered:

$$\frac{1}{E\left\{\frac{1}{\alpha_i}\right\}} \ge \alpha \tag{5}$$

with $i = 1,...,N_U^x$ and α_i is the spectral efficiency of the user i.

3.3 Description of coverage constraints

To serve the users based on their traffic requirements, the coverage constraint can be formulated as:

$$P(\gamma_{i\,j^*}, \gamma_{t\,h}) \le \tau \tag{6}$$

in which:

- $\gamma_{i\,j}$ is the SINR of user i that receives the service from UAV-BS j
- j* is the UAV-BS that offers the highest signal to the user:

$$i, j^* = \arg\max_{x}(\gamma_{i\,j^*}) \tag{7}$$

- $\gamma_{t\,h}$ represents the minimum SINR level required for each user

An area can be considered entirely covered when τ percent of N_U^x users is covered. The user's SINR in the DL and UL can be calculated as proposed in [32]:

$$\gamma_{j^*i}^{(DL)} = \frac{P_{r(j^*i)}^{(DL)}}{\sum_{j=1, j\neq j^*}^{N_{BS}^{x}} P_{r(ji)}^{(DL)} + N} \tag{8}$$

$$\gamma_{j^*i}^{(UL)} = \frac{P_{r(i\,j^*)}^{(UL)}}{\sum_{j=1, j\neq j^*}^{N_{BS}^{x}} P_{r(i\,j)}^{(UL)} + N} \tag{9}$$

in which:

- By denoting the noise power with N_0 as the white noise density, BW as the signal bandwidth, and F as the noise figure, we have:

$$N = N_0 \cdot BW \cdot F \tag{10}$$

- $P_{r(j^*i)}^{(DL)}$ and $P_{r(i\,j^*)}^{(UL)}$ denote the power received in DL (BS to Ground User) and the power received in UL (Ground User to BS).

The power received is given by:

$$P_r^{(z)} = P_t^{(z)} + G_t^{(z)} + G_r^{(z)} - L_{dB} \tag{11}$$

in which:

- The parameter z can be changed by *DL* or *UL*
- P_t is the transmit power
- G_t and G_r represent the transmitter and receiver antenna gain
- L_{dB} is the path loss of the channel

A binary variable is introduced to denote the state of a user i:

$$\beta_i = \begin{cases} 1, & \text{if the user } i \text{ is covered by one } UAV-BS \\ 0, & \text{otherwise} \end{cases} \tag{12}$$

Thus, the following condition must be met to consider the area to be entirely covered:

$$\sum_{j=1}^{N_U^x} \beta_i \geq N_U^x \tau \tag{13}$$

Furthermore, parameter ρ_j will be considered as a vector that contains the state of each UAV-BS, as shown in the following equation:

$$\rho_j = \begin{cases} 1, & \text{if } UAV-BS\ j \text{ is deployed} \\ 0, & \text{if } UAV-BS\ j \text{ is redudant} \end{cases} \tag{14}$$

Finally, the expression of the optimization problem is given as follows:

$$\min_{x,y,h,\rho} \sum_{j=1}^{N_{BS}^x} \rho_j \tag{15}$$

subject to:

$$\sum_{j=1}^{N_{BS}^x} N_{uBS} \varepsilon_{j,s}(x_j, y_j, h) \geq \xi A_s D_s \tag{16}$$

with s=1,…,N_s and also:

$$\sum_{i=1}^{N_U^x} \beta_i(x_i, y_i) \geq N_U^x \tau \tag{17}$$

The UAV-BS cell planning method is presented in the following section based on the developed optimization technique.

4. CELL PLANNING METHODOLOGY

Finding the optimal locations for the UAV-BSs while ensuring the coverage of almost all ground users and achieving their traffic requirements is a complex problem. Moreover, adding the variable altitude of the aerial base stations brings more intricacy to the problem. In this study, we optimize the 3-D placement of the UAV-BSs by exploiting the optimal solution from the pseudo-random behavior of the PSO algorithm [34] and the GA [36]. When we know the optimal locations for all BSs, we can propose to eliminate eventual redundant BSs while respecting the aforementioned constraints.

4.1 Cell planning using PSO algorithm

The PSO algorithm is an optimization algorithm introduced in [35]. Inspired by how swarming animals seek out food to survive, the algorithm starts by generating populations of pseudo-random solutions and aims to improve the candidate solution according to the defined evaluation or quality function.

4.1.1 Analytical expressions of utility functions

To find an optimal solution, our PSO algorithm has to go through multiple iterations. Referring to the vanilla PSO, each node within the network will be a particle. For each iteration, the optimal solution of each node is its current location and the optimal global solution of all nodes are their respective placement in the space. The trajectory of the node gets updated and refined based on the previous local and global solutions. The steps used in the proposed PSO algorithm are summarized in Figure 3 and the list of notations used in the cellular BS planning

is presented in Table III. The optimal latitude, longitude, and altitude are also referred to as the 3-D placement of each UAV-BS. We can achieve this by continuously maintaining respect of the capacity constraints while reducing the utility function:

$$F_1 = \sum_{i=1}^{N_S} \sum_{j=1}^{N_{BS}^x} (N_{uBS} \varepsilon_{j,s} - \xi A_s D_s) \tag{18}$$

at its minimal value. Thus, the last outputs from the previous iteration are the current optimal solutions, which become the new inputs for the next iteration, targeting an improved solution with a total number of users uncovered at its minimal value.

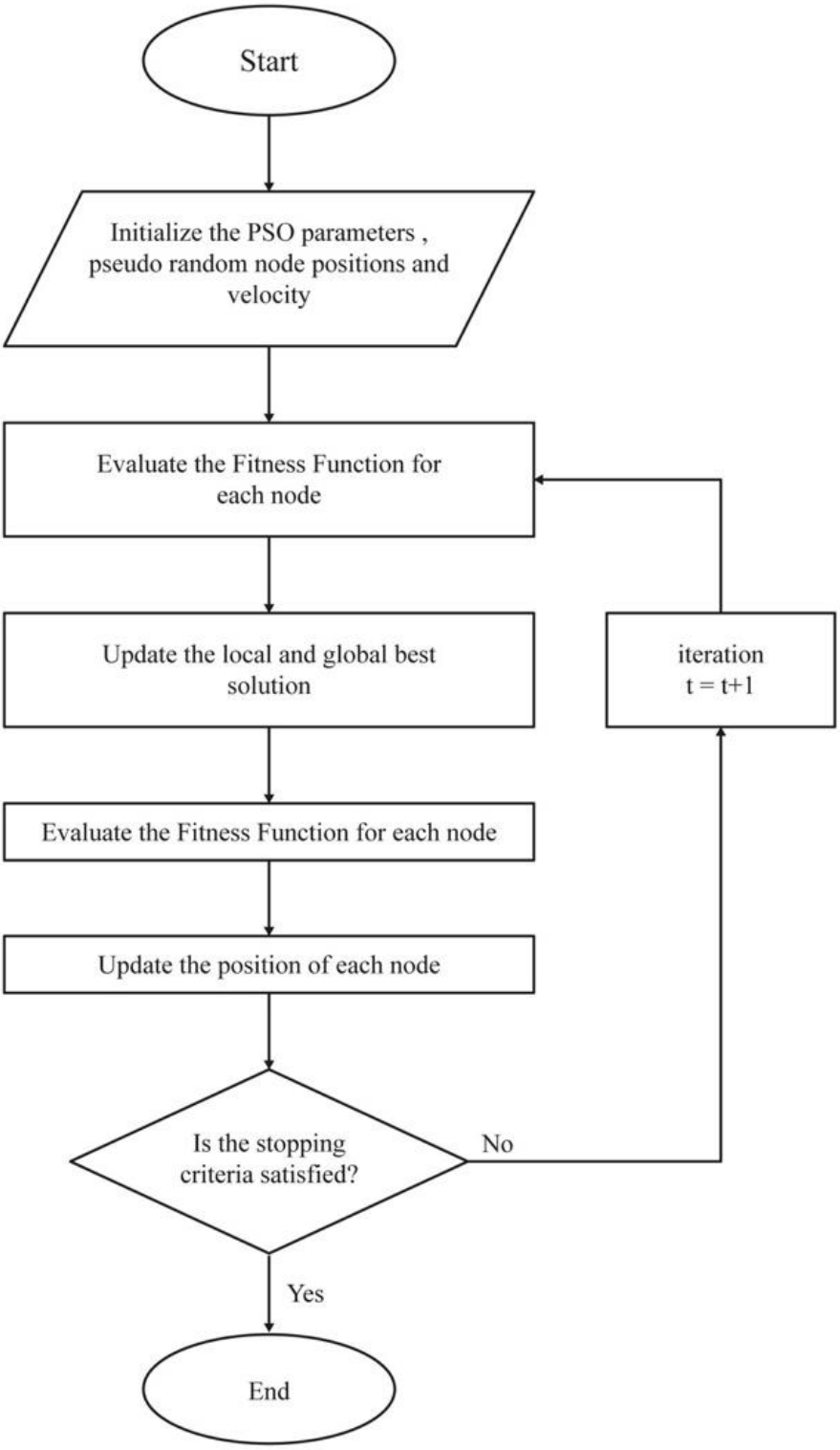

Figure 3 Optimization technique process using the PSO algorithm.

Table III. List of notations for the cell planning using the PSO algorithm

Notation	Description
F_1, F_2	Utility function to satisfy the capacity and coverage constraints
F_3	Utility function to satisfy the average spectral efficiency
W^l	Initial population
$W^{(l,local)}$	Best result of each particle
$W^{(global)}$	Best utility in all iterations
V_φ^l, t	Velocity and iteration
ω	Inertia that controls the convergence speed
c_1, c_2	Personal and global learning coefficients
υ_1, υ_2	Positive random number generated for each j
W_{op}	Optimal solution
σ	Set that contains the UAV-BS j can be eliminated
$\hat{j}$	UAV-BS that can be eliminated

The utility function is given in equation (19) and satisfies the coverage constraint, while keeping the capacity constraint active.

$$F_2 = \begin{cases} -\sum_{j=1}^{N_U^x} \beta_i, & \text{if (4) holds} \\ 0, & \text{otherwise} \end{cases} \tag{19}$$

Finally, the following utility function satisfies the average spectral efficiency of the system:

$$F_3 = \begin{cases} -N_U^x + \alpha - \dfrac{1}{E\left\{\dfrac{1}{\alpha_i}\right\}}, & \text{if (4) holds} \\ 0, & \text{otherwise} \end{cases} \tag{20}$$

4.1.2 PSO process description

The PSO algorithm starts with the generation of L nodes (particles) that have a length of $3N_{BS}^x$ to form the initial population W^l. The pseudo random position of all the UAV-BSs in a given area is held in the vector W^l as follows:

$$W^l = \begin{pmatrix} x^l \\ y^l \\ h^l \end{pmatrix} \tag{21}$$

with l=1,…,L. The optimal result from each node is saved as $W^{(l,local)}$ and the node that offers the best utility in all iterations is kept as $W^{(l,global)}$. From there, $W^{(l,local)}$ and $W^{(l,global)}$ are updated at each iteration (the velocity and movement of the nodes are computed based on them). The velocity V_φ^l, $\varphi = 1,\cdots,N_{BS}^x$ at each iteration t is calculated using the following formula:

$$V_\varphi^l(t+1) = \begin{Bmatrix} \omega V_\varphi^l(t) + c_1\upsilon_1\left[W_\varphi^{(l,local)}(t) - W_\varphi^l(t)\right] \\ +c_2\upsilon_2\left[W_\varphi^{(global)}(t) - W_\varphi^l(t)\right] \end{Bmatrix} \tag{22}$$

in which ω represents the inertia that controls the convergence speed and is generally chosen between 0.8 and 1.2, c_1 and c_2 form the personal and global learning coefficients and υ_1 and υ_2 are two positive pseudo-random numbers generated for each φ. Then, the position of each element φ in W^l is updated based on the following equation:

$$W_\varphi^l(t+1) = W_\varphi^l(t) + V_\varphi^l(t+1) \tag{23}$$

4.1.3 PSO algorithm optimization

The process introduced earlier is repeated until we achieve convergence of the nodes. This state can be reached when the maximum number of iterations is attained. Note that the targets F_2 and F_3 cannot be achieved if the capacity constraint F_1 is not satisfied. Figure 4 presents the pseudocode of the proposed algorithm that aims to find the optimal solution given by $W_{op}=W^{global}$ for the 3-D placement of the UAV-BSs in an area like a stadium to serve τ percent of users based on their data traffic requirements.

Algorithm 1 PSO Algorithm for UAV-BSs deployment

Generate an initial population composed of L random particles $W^l(0)$ of size 3 x N_{BS}^x, $l = 1,...,L$. Set $t = 1$, $F = F_1$, $F^{(global)} = \min\{F^l(0), l = 1,...,L\}$ and $F^{(l,local)} = F^l(0)$.
while $F^{(global)} > -N_U^x$ **do**
  for $l = 1,...,L$ **do**
    Compute $V^l(t)$, $W^l(t)$, $F^l(t)$.
    if $F^l(t) < F^{(l,local)}$ **then**
      $W^{(l,local)} = W^l(t)$, $F^{(l,local)} = F^l(t)$.
      if $F^{(l,local)} < F^{(global)}$ **then**
        $W^{(global)} = W^{(l,local)}$, $F^{(global)} = F^{(l,local)}$.
      end if
    end if
  end for
  if $F^{(global)} \leq 0$ **then**
    $F = F_2$.
  end if
  if $F^{(global)} \leq -\tau N_U^x$ **then**
    $F = F_3$.
  end if
  $t = t + 1$.
end while

Figure 4 Pseudocode of the developed PSO algorithm.

4.2 Cell planning using the GA

The GA is a meta-heuristic algorithm that can provide an effective way to find solutions to complex (non-convex) and large-scale optimization problems [36]. The GA works on a population that consists of specific candidate solutions, where the size of the population is the total number of solutions. Each solution is considered to be a chromosome and each chromosome has a set of genes. The characteristics of the solution represent each gene and each chromosome has a fitness value that is calculated according to the fitness function representing the quality of the chromosome. The GA uses a selection method called the roulette wheel method, in which the chromosome with a higher fitness value has a greater chance of surviving within the population. However, the selection process can only generate the best candidate solution with no additional changes to the chromosomes. To ensure the diversity of the solution and avoid falling into optimal local solutions, crossover and selection are applied after the selection process. In the crossover procedure, two chromosomes are selected in a probability of crossover rate to exchange information so that new chromosomes are generated. Each chromosome has a probability of mutation rate in the mutation procedure to replace a set of genes with new random values.

4.2.1 GA process description

This process repeats for t iteration until t reaches a predefined iteration limit. Figure 5 illustrates the general process of the GA and the notation parameters are presented in Table IV. In this GA model, for UAV-BS j, the combination (x_j, y_j, h_j) is a gene.

Placing genes for all the available UAV-BSs together, i.e., $\{x_j, y_j, h_j\}_{j \in N_{BS}^x}$ gives a chromosome. The required inputs include the total number of iterations (t_{max}), the number of populations in each generation (N_p), the total number of UAV-BSs needed to be deployed at x (day or night) time (N_{BS}^x), the maximum altitude of UAV-BSs (h_{max}), the mutation rate (p_m), and the crossover rate (p_c) for the GA, respectively.

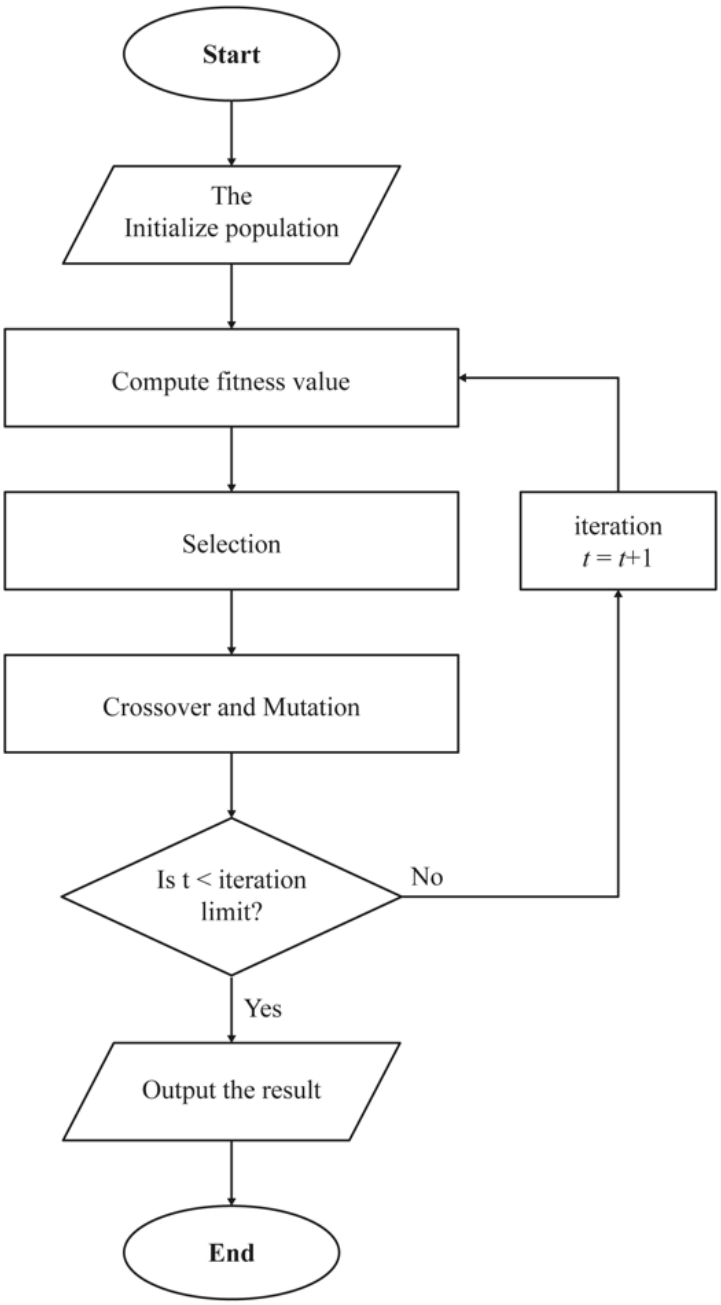

Figure 5 Optimization technique process using the GA.

Table IV. List of notations for the cell planning using the GA

Notation	Description
t	Iteration index
t_{max}	Total number of iterations
N_p	Population size
h_{max}	Maximum altitude (in m)
p_m	Mutation rate
p_c	Crossover rate
L	The number of covered users
v	A set of number of users covered by each UAV-BS
$\hat{v}$	A set of total number of users covered by all UAV-BSs
$\hat{i}$	Covered user
κ_1	First population

4.2.2 GA expected output parameters

The outputs are the horizontal locations (x_j, y_j) as well as the altitudes (h_j), denoted by $L_j, j = 1, 2, \ldots, |N_{BS}^x|$, of all the UAV-BSs. First, $|N_{BS}^x|$ empty lists are created and each of them is used to store the covered users of the corresponding UAV-BS. Then, two arrays (v and $\hat{v}$) are created to store the number of users covered by each UAV-BS and the total number of users covered by all UAV-BSs, known as the fitness score. The first population (κ_1) is generated by the creation of N_p chromosomes, in which the horizontal locations of all UAV-BSs are initialized by assigning each of them with the equidistant point of three random user locations, while the altitude of the UAV-BSs is initialized by generating random numbers between 100 and h_{max}. The process continues with the application of the conditions of association between UAV-BSs and users. In our study, if the user receives a SINR (γ_{ij}) greater than the SINR threshold (γ_{th}), the user can be associated with the UAV-BS transmitter and the number of covered users $|L_j|$ is stored in an array (v). Otherwise, if the γ_{ij} received is less or equal to γ_{th}, the user cannot be served by the UAV-BS transmitter and a negative number must be stored in the array $\hat{v}$, referring to a negative fitness value for this chromosome. The fitness function of the chromosome is the total number of covered users saved into the array. Next, the roulette wheel method is applied to update the current population (κ_t) and a random chromosome is chosen from within the current population to be the competitor. By comparing the fitness score of all chromosomes with the competitor, the chromosomes with fewer fitness scores are replaced with the competitor. Thereafter, in the crossover procedure, p_c chromosomes are randomly selected and paired. Each pair is considered to be a parent chromosome. In each parent chromosome, genes from the first half of one chromosome and genes from the second half of the other chromosome are exchanged to produce the children's chromosomes. All chromosomes have a p_m probability of performing a mutation process in which a mutated chromosome gene is selected to be replaced by random horizontal locations and altitudes.

4.2.3 GA implementation

At this stage, we can obtain the result of the horizontal locations and the altitudes of aerial BS by choosing the chromosomes with the maximum fitness scores. Figure 6 displays the algorithm for UAV-BS deployment based on the proposed GA.

Algorithm 2 Genetic Algorithm for UAV-BSs deployment

Input: $t_{max}, N_p, N_{BS}^x, h_{max}, p_m, p_c, \tau, N_U^x, N_s, N_{uBS}, \xi, D_s, A_s$
Output: $x_j, y_j, h_j, \{j \in N_{BS}^x\}$
Create $|N_{BS}^x|$ empty list. $\{\mathscr{L}_j\}_{j \in N_{BS}^x}$
Create two arrays v, $\hat{v}$ with size $|N_{BS}^x|$ and N_p respectively.
Initialize Population: Initialize first population κ_1 by creating N_p sets of chromosomes.
for $t = 1; t \leq t_{max}; t = t + 1$ **do**
  for $\hat{i} = 1; \hat{i} \leq N_p; \hat{i} = \hat{i} + 1$ **do**
    Perform the user assignments $\sum_{i=1}^{N_U^x} \beta_i(x_i, y_i) \geq \tau N_U^x$ according to the SINR received from the UAV-BS and store the results in $\{\mathscr{L}_j\}_{j \in N_{BS}^x}$.
    for $j = 1; j \leq |N_{BS}^x|; j = j + 1$ **do**
      if $\sum_{i \in \mathscr{L}_j} \gamma_{ij} > \gamma_{th}$ **then**
        $v[j] \longleftarrow |\mathscr{L}_j|$
      else
        $\hat{v}[\hat{i}] \longleftarrow -N_p$
        Continue and go back to step 5
      end if
    end for
    Fitness Function: $\hat{v}[\hat{i}] = sum(v)$
  end for
  Selection: Update κ_t using roulette wheel method to select chromosomes
  Crossover: Based on p_c, update κ_t by exchanging information of parent chromosomes to produce children chromosomes
  Mutation: Based on p_m, genes are selected and replaced by new values randomly
end for
Find the chromosome with maximum value in $\hat{v}$ and obtain $\{x_j\}_{j \in N_{BS}^x}$ and $\{y_j\}_{j \in N_{BS}^x}$ from the chromosome.
Obtain $\{h_j\}_{j \in N_{BS}^x}$ by solving $\sum_{s=1}^{N_s} \sum_{j=1}^{N_{BS}^x} \{N_{uBS} \varepsilon_{j,s}(x_j, y_j, hj) - \xi D_s A_s\}, \frac{1}{E\{\frac{1}{\alpha_i}\}} \geq \alpha$
return $\{x_j\}_{j \in N_{BS}^x}, \{y_j\}_{j \in N_{BS}^x}, \{h_j\}_{j \in N_{BS}^x}$

Figure 6 Pseudocode of the developed GA.

4.3 Discarding the redundant UAV-BS

At this stage, we have defined the 3-D placements of the UAV-BSs. In order to avoid redundancy, we must discard UAV-BSs whose absence does not negatively impact the capacity and coverage constraints. In other words, if a UAV-BS is discarded from the nodes and one of the optimization problem constraints is affected negatively by its absence during the simulation, we should keep that UAV-BS as it is considered indispensable for the operation of the network. To achieve this objective, we have to optimize the binary vector ρ_j and find the optimal UAV-BS combination while respecting the performance of Algorithm 1 presented in the earlier sections. This process starts by considering that all UAV-BSs are deployed in the target area ($\rho(t) = [1, \ldots, 1]$). From there, we eliminate the UAV-BSs one by one and, for each, verify whether the problem constraints are still satisfied or not. If a UAV-BS j causes a degradation of the general performance, it cannot be discarded ($\rho_j = 1$). Otherwise, the algorithm will assume that UAV-BS j can be removed and placed in set σ. After checking all the UAV-BSs, the algorithm will only focus on set σ to find those UAV-BSs that can be safely eliminated before establishing their corresponding value in from ρ_j to 0. Among all the UAV-BSs in set σ, only the ones with the smallest impact on the number of served users can be eliminated. These UAV-BSs will be denoted $\hat{j}$ and obtained by using the following equation:

$$\hat{j} = \arg\max_{j\in\sigma} \sum_{i=1}^{N_S} \sum_{j=1, j\neq\hat{j}}^{N_{BS}^x} \left\{ N_{uBS} \varepsilon_{j,s}(W_{op}) - \xi A_s D_s \right\} \tag{24}$$

with s=1,…,N_s. This procedure will be repeated with the UAV-BSs in σ until the UAV-BS combination is obtained. Algorithm 3 as shown in Figure 7 elaborates on the details of how the redundant UAV-BSs are discarded from the nodes.

Algorithm 3 Iterative Algorithm to eliminate the redundant UAV-BSs

$t = 0$.
Assume that all UAV-BSs are deployed $\rho(t) = [1, \ldots, 1]$.
repeat
  for $j = 1, \ldots, N_{BS}^x$ **do**
    if $\sum_{j=1}^{N_{BS}^x} N_{uBS} \varepsilon_{j,s}(x_j, y_j, h_j) \geq \xi D_s A_s$ **then**
      if $\frac{1}{E\{\frac{1}{\alpha_i}\}} \geq \alpha$ **then**
        if $\sum_{i=1}^{N_U^x} \beta_i(x_i, y_i) \geq \tau N_U^x$ **then**
          $j \in \sigma$. ▷ UAV-BS j can be eliminated.
        else
          $j \notin \sigma$. ▷ UAV-BS j cannot be eliminated.
        end if
      end if
    end if
  end for
  $\hat{j} = \arg\max_{j\in\sigma} \sum_{s=1}^{N_s} \sum_{j=1, j\neq\hat{j}}^{N_{BS}^x} \{N_{uBS} \varepsilon_{j,s}(W_{op}) - \xi D_s A_s\}$.
  $\sigma = \sigma \setminus \{\hat{j}\}$,
  $\rho(t+1) = \rho^{\hat{j}}(t)$. ▷ UAV-BS $\hat{j}$ is eliminated safely.
  $t = t + 1$.
until $\sigma = \varnothing$.

Figure 7 Pseudocode of the developed algorithm with redundant UAV-BS elimination.

4.4 Concluding remark on the two proposed planning methods

Planning the placements of the UAV-BSs is an important step that must be taken before the devices can be deployed. This research focuses on using UAV-BSs to cover a stadium-sized area during some events. To achieve this goal, this report begins by defining the system model using a definition of the air-to-ground channel model that considers both LoS and NLoS [37]. In addition to the usual parameters that must be considered in the deployment of BTSs, the type of UAVs and their autonomy must be taken into account when considering the

deployment of UAV-BSs. Low-altitude platforms are suggested as they can fulfill the requirement of longer flying time while having enough altitude to be used as an aerial BS. We described the optimization problem that considers both the coverage and capacity constraints as well as the average spectral efficiency of the system in order to serve the ground users based on their QoS and traffic requirements. Two different methods, namely the PSO algorithm and GA were formulated to find the optimal 3-D placements for the UAV-BSs. Overall, overlapping tasks in the working area and signal redundancy from the deployed UAV-BSs have been addressed while maintaining the restrictions put forward earlier.

5. CASE STUDY AND SIMULATION DESCRIPTION

The overall objective of this work is to provide network coverage to a stadium-sized area during an event using UAV-BSs. We used the GA and PSO algorithm to determine the minimum number of UAV-BSs needed to serve the users based on their traffic requirements. We built the scheme while considering both the capacity and coverage constraints as well as the average spectral efficiency.

5.1 Case study parameters

This section reports and evaluates the results of the multiple simulations performed in order to verify the proposed approaches' effectiveness and performance in the remaining part of the paper. This case study assumes that the stadium size to cover with the network is a rectangular stadium of 1000 × 100 m². The ground users that must be served can either sit or stand; nonetheless, we assume a total of 1,000 users can be covered in the area. However, for most events requiring the use of the area, most users are seated, thus nearing the site's edges, and only a few remain within the center of the field. This results in the creation of clusters; thus, we deliberately divided the area into inner and outer subareas. For the remainder of this experiment, we set the ground user density within the inner area to 10% of the total users. The remaining 90% are all scattered throughout the outer area. We also assume that the UAV-BS in this simulation is equipped with omni-directional antennas to allow for full 3-D connectivity. The UAV-BS cellular network system will be simulated in this experiment using the MATLAB® environment and the parameters are presented in Table V. Additionally; Table VI presents the considered DL and UL parameters. To provide a diverse report overview in this simulation, we present two types of scenarios. The first is when the area to cover contains all 1,000 ground users that must be served within the network and the second scenario is when the number of the users is a bit lower (with only 60% of our total pre-defined ground users).

Table V. Simulation Parameters

Environment Parameter	Value	Environment Parameter	Value
a	9.61	h_{max}	600 m
b	0.61	p_c	0.08
η_{LoS}	1	γ_{th}	-7 dB
η_{NLoS}	20	N_0	-174 dBm/Hz
t_{max}	100	F	5 dB
p_m	0.01	V_{max}	500 m
f_c	2 GHz	N_p	12
α	30 bps/Hz	L	12 dB
BW	100 MHz	p_c	0.08
ξ, τ	98%	γ_{th}	-7 dB

Table VI. DL and UL parameters

DL Parameter	Value	UL Parameter	Value
R^{DL}	100 Mbps	R^{UL}	50 Mbps
P_t^{DL}	49 dBm	P_t^{UL}	23 dBm
G_t^{DL}	17.5 dB	G_t^{UL}	0 dB
G_r^{DL}	0 dB	G_r^{UL}	17.5 dB

The present subsection discusses the application case associated with simulation results of the UAV-BS deployment during the day.

5.2 First case scenario: dense ground users

As described earlier, there are 1,000 ground users that must be served within the area of interest in this first case. The initial number of UAV-BSs at the start of the simulation is set to 34. The ground users are scattered within the area to cover, but we still keep two clusters and the subareas shown in Figure 8. The blue dots represent the ground users. Considering the stadium's geometry, only a small percentage of the users are in the central area (subarea 1), as most of them are located in the seating zone of the stadium.

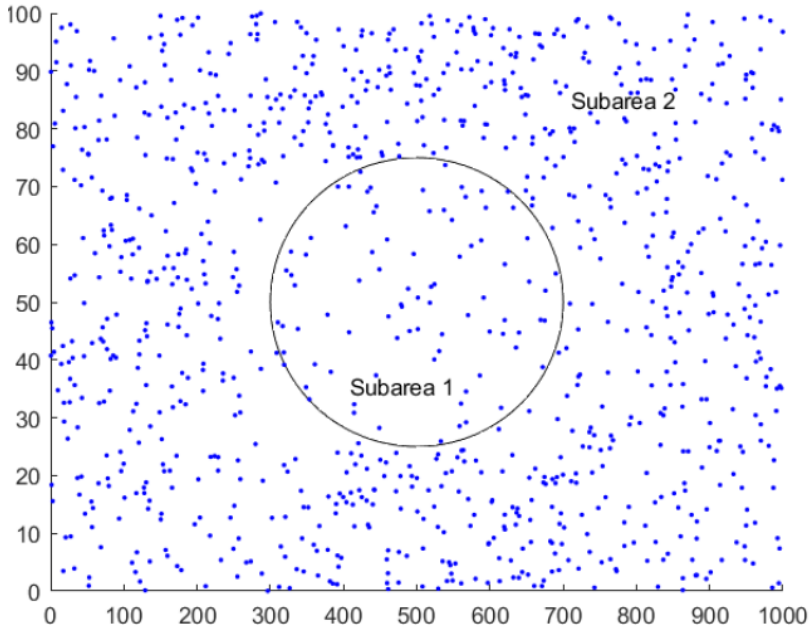

Figure 8 Distribution of users during the first case study.

5.2.1 Deployments simulation of the UAV-BSs using the PSO algorithm and GA

As mentioned earlier; to serve these users based on the capacity and coverage constraints as well as the average spectral efficiency, we must experiment with the deployments of the UAV-BSs using two methods. The first uses the PSO algorithm presented in Figure 9. The steps of that algorithm are detailed in Figure 10.

The algorithm applies the following settings: the initial population size L is set to 12 and the velocity $V^{l}_{\varphi} \in [-V_{max}, V_{max}]$ with V_{max} is the maximum achieved velocity. To limit the movement of UAV-BSs from one iteration t to another, we choose $V_{max} = 500$ m. F_1 is the utility function that satisfies the capacity constraint and finds the 3-D locations of the UAV-BSs. The utility functions F_2 and F_3 satisfy the coverage constraint and the average spectral efficiency while maintaining the capacity constraint. The second phase of the experiment was to use the GA presented in Algorithm 2 (Figure 5) to find the 3-D placements of the UAV-BSs. The settings applied to the GA in order to achieve this goal are as follows: the initial population size N_p is set to 12, the iteration limit t_{max} is fixed to 100, and the mutation rate p_m and the crossover rate p_c are configured to 0.01 and 0.08, respectively. Figure 10 presents this process followed by the GA.

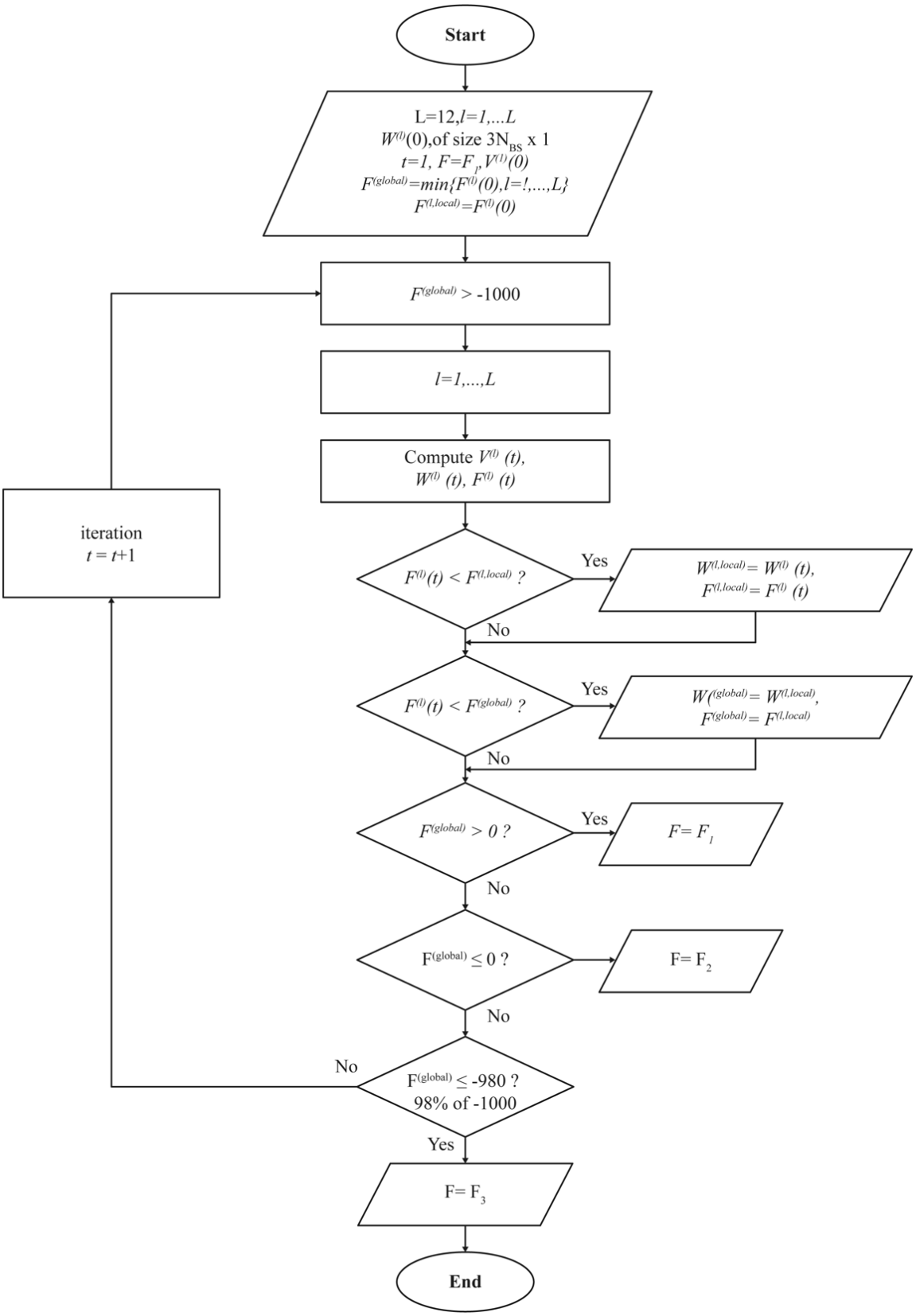

Figure 9 UAV-BSs deployment process with the PSO algorithm.

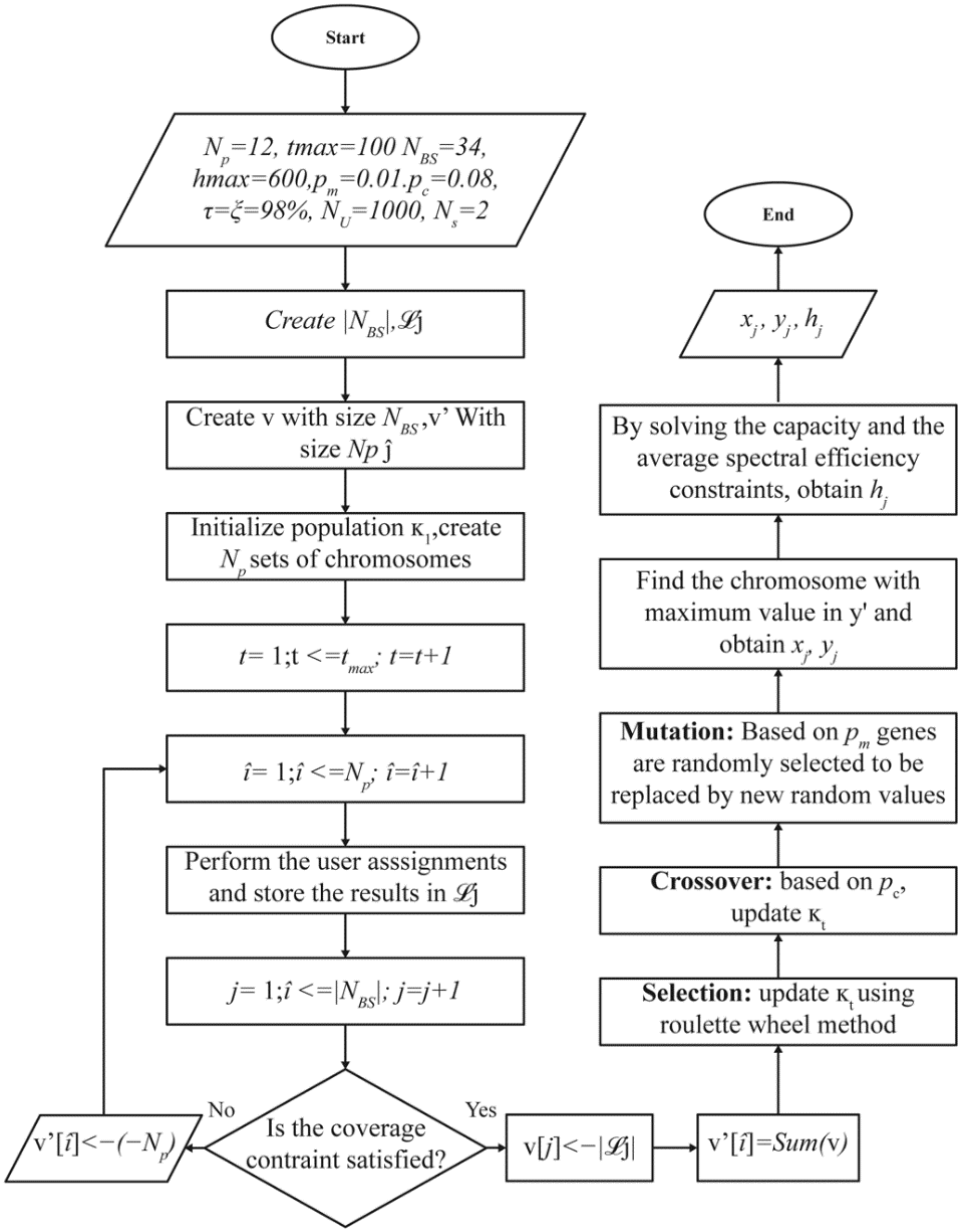

Figure 10 UAV-BSs deployment process with the GA.

5.2.2 Redundant UAV-BS elimination

After finding the 3-D locations of the UAV-BSs by using either the PSO algorithm or the GA, we introduce a third algorithm in Figure 11 for discarding redundant BSs from the deployment. Based on our experiments, the final number of UAV-BSs required to serve all the ground users is different depending on whether the PSO algorithm or GA was used. From the PSO algorithm, the number of UAV-BSs required is 33. Among the 34 UAV-BSs proposed in the initial stage, one BS was identified as redundant. From the GA, all 34 UAV-BSs were identified as essential for deployment in order to serve the ground users.

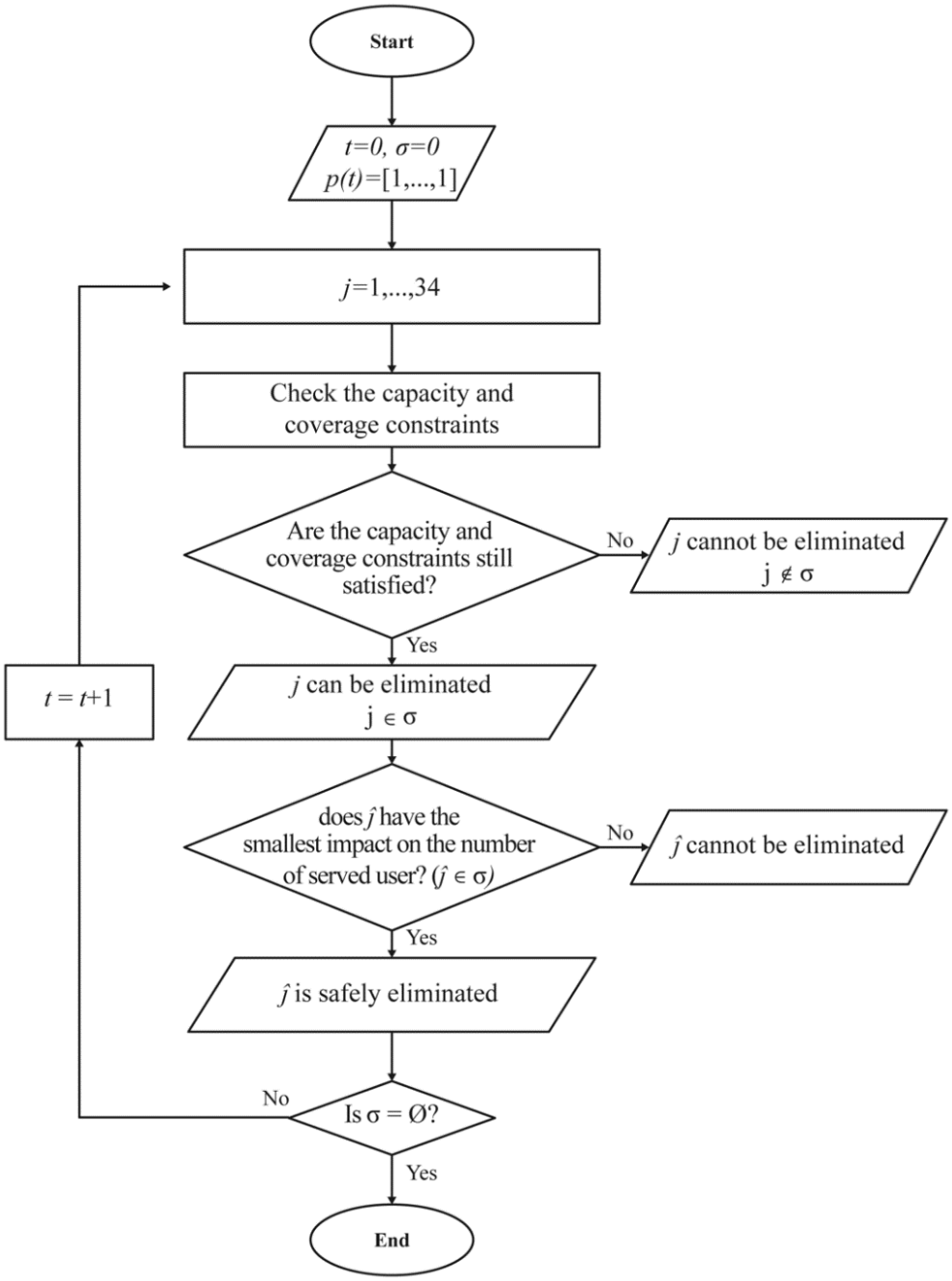

Figure 11 Redundant UAV-BSs elimination process.

5.2.3 UAV-BS deployment simulation

In Figures 12, we report the 2-D projection of the UAVs placements and the distribution of the users within the studied area. The red and magenta triangle shape represent the UAV-BSs. The red UAV-BSs (mostly in the center) are tasked to cover subarea 1, whereas the UAV-BSs colored in magenta are tasked to cover subarea 2 (the outer region). The figure makes it easy to see the disproportion of the user density of the inner and outer areas. Thus, making it clear that more UAV-BSs are required to cover this outer area in order to satisfy the ground users' downlink and avoid congestion.

DOI: https://doi.org/10.37256/cnc.3220257142

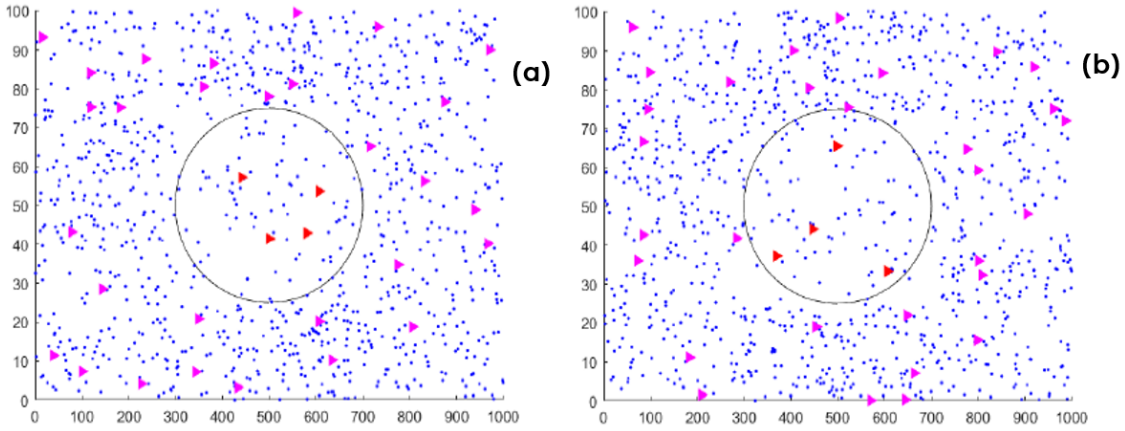

Figure 12 2-D projections of UAV-BSs locations and ground users' distribution from the deployments using (a) PSO algorithm and (b) GA.

5.2.4 Deployment of 2-D and 3-D distribution and SINR of the UAV-BS

The association policy between users and the UAV-BSs is based on the best SINR. As a result, the coverage and altitude of the UAV-BSs are different for the PSO algorithm and GA, as shown in Figures 13. The 3-D locations of the UAV-BSs in Figures 13(a) and 13(b) indicate that, in subarea 2, which has a higher density of ground users, the average altitude of the UAV-BSs is lower than in subarea 1. Thus, a densely populated area with ground users requires more UAV-BSs. However, to avoid interference when servicing ground users and avoid competition between the drones, which will result in a decrease in the general network, UAV-BSs that compete with other UAV-BSs knowing that the nearby ground users are already served by others, should decrease their altitude to reduce their coverage radius and minimize interference. In the central area (subarea 1), where the user density is lower, the UAV-BSs tend to increase their altitudes to decrease the path loss and cover more ground users in the area.

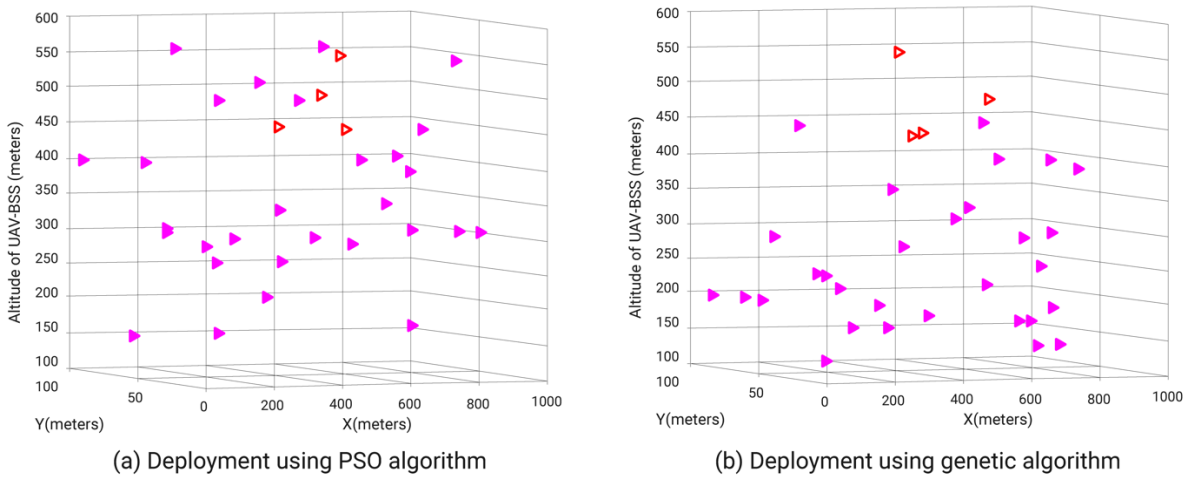

Figure 13 3-D locations of UAV-BSs from the deployments using (a) PSO algorithm and (b) GA.

5.2.5 Comments on the simulation performance

To determine the quality of service and the performance of the system, the cumulative distribution function (CDF) of the SINR when deployments were assessed based on the use of the PSO algorithm and GA, respectively. When the SINR received by the ground user is less than or equal to -7 dB, the probability of having an association between that ground user and the UAV-BSs transmitter is 0. However, when the SINR received increases, the probability of having an association between the UAV-BS and the ground user also increases. The performance of the PSO algorithm compared to the GA is illustrated in Figure 14. In the deployment targeted τN_U^{Day} with 980 simulated ground users, representing 98% of the total ground users within the studied area, the PSO algorithm

was compared to the GA and reached the target at the 22nd iteration, whereas the GA needed until the 44th iteration to meet the target.

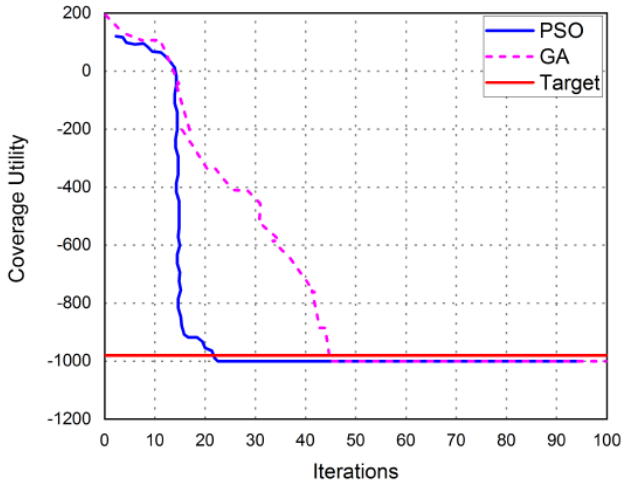

Figure 14 Convergence speed of the PSO algorithm and GA.

It should be noted that, in the PSO algorithm, the coverage utility is equal to the utility function F_1 when F_1 is greater than zero. However, for negative values of F_1 and if the utility function F_2 is greater than $-\tau N_U^{Day}$, the coverage utility is equal to F_2; otherwise, it is equal to the utility function F_3.

5.3 Second case: fewer ground users

The present section discusses the experiments and simulation results of the deployment of UAV-BSs with a reduced number of ground users to serve scattered around the same stadium-sized area. Thus, in our setup, we initially estimated that 20 UAV-BSs are needed to serve 600 ground users. Similar to the setup in the first case, the placements of the ground users are scattered throughout the target area.

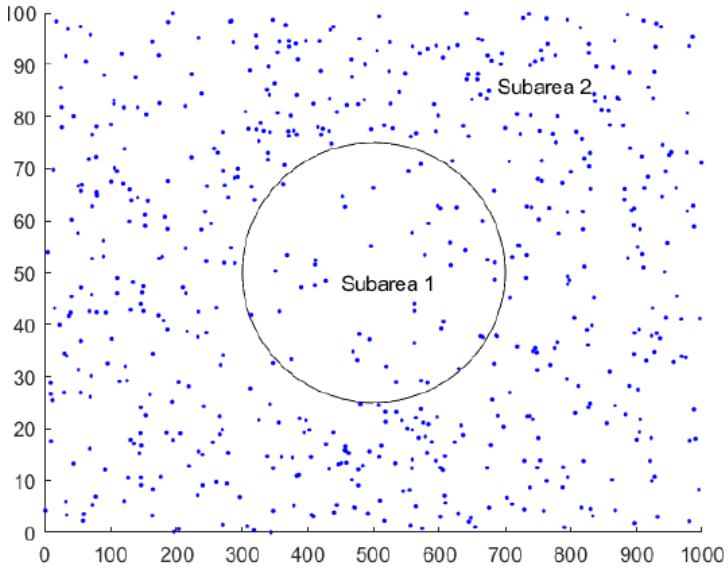

Figure 15 Distribution of users based on the second case study.

10% are distributed in subarea 1, whereas 90% are distributed in subarea 2. Figure 15 presents a visual of our initial setup.

5.3.1 Deployments simulation of the UAV-BSs using the PSO algorithm and GA

The deployments simulation of the UAV-BSs using the PSO algorithm and GA follows the same process and parameters as we introduced in the first case. Thus, aside from the initial number of ground users and the

estimated UAV-BSs used in the PSO algorithm and GA, the next step is to find the 3-D placement of the UAV-BSs and eliminate the redundant BSs. In Figure 16, the blue dots represent the ground users, while the red and magenta triangles represent the UAV-BSs in subareas 1 and 2, respectively. The outcome in terms of performance for both the PSO algorithm and GA is presented in Figures 16 and 17. The PSO algorithm and GA both require 20 UAV-BSs to cover the specified area. The central area (subarea 1) only has 2 UAV-BSs scattered away from each other compared to the other UAVs in subarea 2, which has a higher density of ground users to serve. Looking at the altitude of the UAV-BSs, the same pattern we had introduced in the first case is kept. Meanwhile, in the subarea with higher user density, we have generalized UAV-BSs flying at a lower altitude. This can be explained as the optimization objective's outcome targeted at reducing overlap that causes interference.

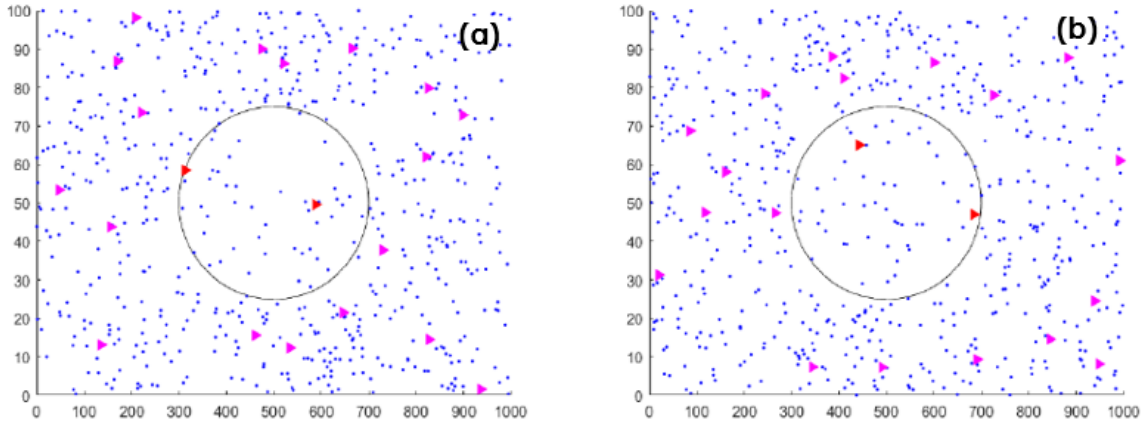

Fig. 16. 2-D projection of UAV-BSs placements and ground user distribution from deployments using (a) PSO algorithm and (b) GA.

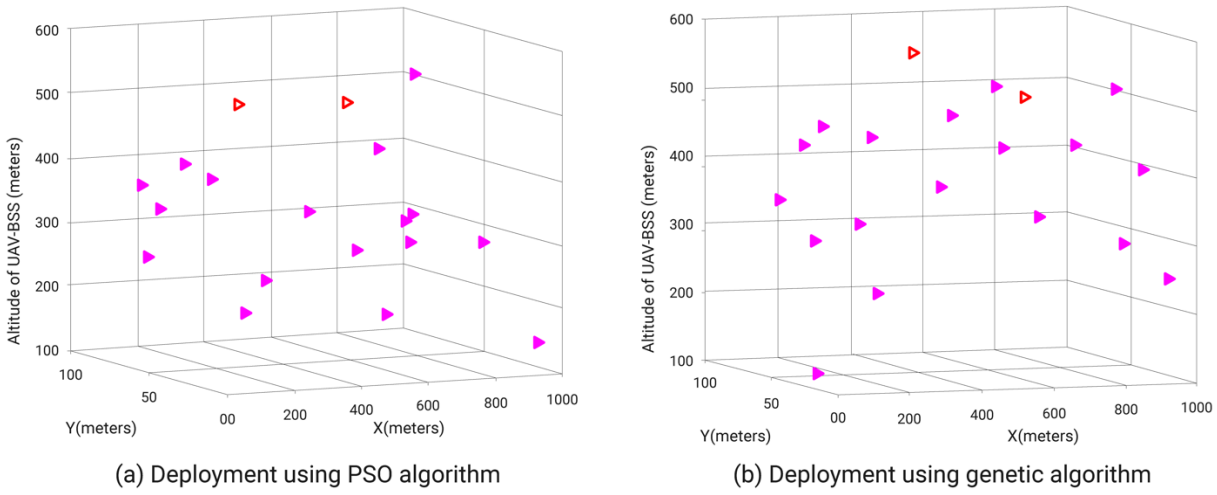

Fig. 17. 3-D locations of UAV-BSs from the deployments using (a) PSO algorithm and (b) GA.

5.3.2 Discussion on SINR and convergence performances

For the QoS and the system's performance, the SINR distribution, reflecting the probability of association between a user and a UAV-BS transmitter if the user receives an SINR higher than -7 dB. The convergence speed of the PSO algorithm was also compared to the GA during our simulation deployment for this second case. The target τN_U^{Night} is 588, representing 98% of the total ground users for this second simulation. Similar to our outcome in the first simulation, the PSO algorithm performed faster than the GA and achieved the target at the ninth iteration, whereas the GA requires 30 iterations to do the same.

5.4 State of the art on the UAV-BS optimization algorithm

The internet access allowing customers to post photos on social media and streaming video has become important in a complex urban environment [38-39]. Few recent years ago, the use of UAVs in wireless communications has attracted widespread attention. To meet these needs, a ground BS is not an appropriate solution because when there is no sporting event, there is a high probability that the BS will have only a few loads or will have no charge. In this case, using UAVs as BSs with appropriated optimization planning method as developed in the present paper is a suitable solution.

Different algorithms were proposed to optimize the UAV-BS, for example, to reach a precise monitoring with trajectory planning in the urban environment [40]. A concept of multi-layer operation of UAV-BS cellular network was proposed [41]. It acts as an intelligent deployment of UAVs in 5G heterogeneous communication environment for improved coverage. A survey and various protocols of classification and associated architectures UAV assisted 5G and beyond wireless networks were proposed [42]. An overview on reinforcement learning algorithms and planning wireless cellular networks can be found in [43-45].

During an emergency or disaster situation, a drone can be used as a BS if the ground installation is destroyed or if the required services are not available. The UAVs can also be used as trunks where some improvements are required for the performance of existing networks. Using a drone as a wireless communication node as a relay or BS can reduce operating costs. Besides, deploying UAV-BS is simpler and more flexible than traditional BS. Nowadays, research work enabling to plan the deployment of UAV-BSs for sporting events in 5G cellular networks is needed. Then, the performance of the use of UAVs as BSs should be evaluated. Research work aiming to serve wireless network users at sports events through UAV-BSs and having main objective to maximize network revenues is needed. Based on the present study more than hundred drone BSs can optimally serve users based on their traffic and QoS requirements under challenging items:

- Determining the minimum number of drone-BS that can cover a stadium and,
- Identifying the capacity constraint, coverage constraint, and 3-D placement of UAV-BS by providing a heuristic algorithm based on problem optimization.

6. DISCUSSION, CONCLUSION AND FUTURE WORK

In this work, we present the use and planning of UAVs as base stations while minimizing the number of devices deployed and covering the requirement coverage given the predefined stadium-sized area. We achieved this goal and were able to serve the ground users with their traffic requirements. The defined optimization problem considered the capacity and coverage constraints as well as the average spectral efficiency of the system. We used and compared the performance of both PSO and GA on their ability to provide a reliable, usable, and effective solution in finding the 3-D placement of the UAV-BSs. To be efficient, we reduced the number of drones to deploy to the minimum required by discarding the UAV-BSs judged to add redundancy to the network. However, we ensured that UAV-BSs discarded from the nodes did not negatively affect the coverage or network quality. We experimented and simulated the proposed deployment planning with different parameters and the number of ground users to be served. Considering the UAV-BSs are positioned according to the solutions' 3-D coordinate placements and the ground users connected to them are serving the highest suitable signal, the CDF of the SINR shows that these approaches satisfy the quality of the service required. The PSO algorithm performed faster and better when compared to the GA and has proven to provide acceptable solution performance proportional to the number of ground users that need to be served and the area that needs to be covered. In a nutshell, the approach based on the PSO algorithm is an efficient and feasible method to deploy UAV-BSs that satisfies the coverage and capacity constraints while achieving a good target QoS in the next generation of the network.

The present research introduces some promising concepts for the future generation of wireless network technology. The future study by developing the proposed simulation will take into account deeper analysis, like studying signal fading, energy-speed trade-offs, atmospheric turbulences [46-47] and real-world rules. As ongoing research, we are working on developing the UAV-BS operation for the elaboration of multi-beam steering by using negative group delay (NGD) based stair phase shifters as introduced in [48-49] to overcome issues related to the latency and signal propagation delay [50]. In the future, we aim to use this work as a foundation to produce a UAV-BS innovative NGD equalization technique with delay synchronization [51-52].

Acknowledgments

This research work was supported by National Natural Science Foundation of China (NSFC) Grant No. 61750110535 and also supported by the Chinese government through the Chinese Scholarship Council (CSC).

Conflict of Interest

There is no conflict of interest for this study.

REFERENCES

[1] Zaher D, Saad W, Ghosh A, Andrews JG, Yaacoub E. Toward massive machine type cellular communications. *IEEE Wireless Communications*. 2016; 24(1): 120-128.

[2] Haider F, Wang C-X, Haas H, Yuan D, Wang H, Gao X, You X-H, Hepsaydir E. Spectral efficiency analysis of mobile femtocell based cellular systems. *Proceedings of 2011 IEEE 13th international conference on communication technology*, *Jinan, China*. 2011. p. 347-351.

[3] Zanella A, Bui N, Castellani A, Vangelista L, Zorzi M. Internet of things for smart cities. *IEEE Internet of Things journal*. 2014; 1(1): 22-32.

[4] Miranda J, Cabral J, Wagner SR, Pedersen CF, Ravelo B, Memon M, Mathiesen M. An open platform for seamless sensor support in healthcare for the internet of things. *Sensors*. 2016; 16(12): 2089. 2-22.

[5] Miranda J, Memon M, Cabral J, Ravelo B, Wagner SR, Pedersen CF, Ravelo B, Memon M, Mathiesen M, Nielsen C. Eye on patient care: Continuous health monitoring: design and implementation of a wireless platform for healthcare applications. *IEEE Microwave Magazine*. 2017; 18 (2): 83-94.

[6] Pankaj S. Evolution of mobile wireless communication networks-1G to 5G as well as future prospective of next generation communication network. *International Journal of Computer Science and Mobile Computing*. 2013. 2(8): 47-53.

[7] Arshad QKUD, Kashif AU, Quershi IM. A review on the evolution of cellular technologies. *Proceedings of 2019 IEEE 16th International Bhurban Conference on Applied Sciences and Technology*, *IBCAST*, Jan 2019. p. 989-993.

[8] Bohli A, Bouallegue R. How to meet increased capacities by future green 5G networks: A survey. *IEEE Access*. 2019. 7: 42220-42237.

[9] Kalra B, Chauhan DK. A comparative study of mobile wireless communication network: 1G to 5G. *International Journal of Computer Science and Information Technology Research*. 2014. 2(3): 430-433.

[10] Jain VS, Jain S, Kurup L, Gawade A. Overview on Generations of Network: 1G, 2G, 3G, 4G, 5G. *IOSR Journal of Electronics and Communication Engineering*, 2014. 9(3): 1789-1794.

[11] Meraj M, Kumar S. Evolution of mobile wireless technology from 0G to 5G. *International Journal of Computer Science and Information Technologies*. 2015. 6(3): 2545-2551.

[12] Nguyen HC, Amorim R, Wigard J, Kovács IZ, Sørensen TB, Mogensen PE. How to ensure reliable connectivity for aerial vehicles over cellular networks. *IEEE Access*. 2018. 6: 12304-12317.

[13] Bauschert T, Büsing C, D'Andreagiovanni F, Koster AM, Kutschka M, Steglich U. Network planning under demand uncertainty with robust optimization. *IEEE Communications Magazine*. 2014. 52(2): 178-185.

[14] Yang N, Wang L, Geraci G, Elkashlan M, Yuan J, Di Renzo M. Safeguarding 5G wireless communication networks using physical layer security. *IEEE Communications Magazine*. 2015. 53(4): 20-27.

[15] Liu D, Wang L, Chen Y, Elkashlan M, Wong K-K, Schober R, Hanzo L. User association in 5G networks: A survey and an outlook. *IEEE Communications Surveys & Tutorials*. 2016. 18(2): 1018-1044.

[16] Mozaffari M, Saad W, Bennis M, Nam Y-H, Debbah M. A tutorial on UAVs for wireless networks: Applications, challenges, and open problems. *IEEE Communications Surveys & Tutorials*. 2019. 21(3): 2334-2360.

[17] Fotouhi A, Qiang H, Ding M, Hassan M, Giordano L G, Garcia-Rodriguez A, Yuan J. Survey on UAV cellular communications: Practical aspects, standardization advancements, regulation, and security challenges. *IEEE Communications Surveys & Tutorials*. 2019. 21(4): 3417-3442.

[18] Zeng Y, Zhang R, Lim T J. Wireless communications with unmanned aerial vehicles: Opportunities and challenges. IEEE Communications Magazine. 2016. 54(5): 36-42.

[19] Dalamagkidis K. Classification of UAVs. *Handbook of unmanned aerial vehicles*. 2015. p. 83-91.

[20] Alzenad M, El-Keyi A, Lagum F, Yanikomeroglu H. 3-D placement of an unmanned aerial vehicle base station (UAV-BS) for energy-efficient maximal coverage. *IEEE Wireless Communications Letters*. 2017. 6(4): 434-437.

[21] Shakhatreh H, Khreishah A, Alsarhan A, Khalil I, Sawalmeh A, Othman NS. Efficient 3D placement of a UAV using particle swarm optimization. *Proceedings of 2017 IEEE 8th International Conference on Information and Communication Systems*, *IEEE ICICS 2017*, 2017. p. 258-263.

[22] Zeng Y, Zhang R. Energy-efficient UAV communication with trajectory optimization. *IEEE Transactions on Wireless Communications*. 2017. 16(6): 3747-3760.
[23] Clerc M, Kennedy J. The particle swarm-explosion, stability, and convergence in a multidimensional complex space. *IEEE Transactions on Evolutionary Computation*. 2002. 6(1): 58-73.
[24] Bor-Yaliniz RI, El-Keyi A, Yanikomeroglu H. Efficient 3-D placement of an aerial base station in next-generation cellular networks. *Proceedings of 2016 IEEE international conference on communications*, *2016 IEEE ICC*, p. 1-5.
[25] Wang H, Zhao H, Wu W, Xiong J, Ma D, Wei J. Deployment algorithms of flying base stations: 5G and beyond with UAVs. *IEEE Internet of Things Journal*. 2019. 6(6): 10009-10027.
[26] Gupta L, Jain R, Vaszkun G. Survey of important issues in UAV communication networks. *IEEE Communications Surveys & Tutorials*. 2015. 18(2): 1123-1152.
[27] Al-Hourani A, Kandeepan S, Jamalipour A. Modeling air-to-ground path loss for low altitude platforms in urban environments. *Proceedings of 2014 IEEE global communications conference*, 2014. p. 2898-2904.
[28] Matolak DW. Air-ground channels & models: Comprehensive review and considerations for unmanned aircraft systems. *Proceedings of 2012 IEEE aerospace conference*, 2012. p. 1-17.
[29] Matolak DW, Sun R. Air–ground channel characterization for unmanned aircraft systems—Part I: Methods, measurements, and models for over-water settings. *IEEE Transactions on Vehicular Technology*. 2016. 66 (1): 26-44.
[30] Feng Q, Tameh EK, Nix AR, McGeehan J. WLCp2-06: Modelling the likelihood of line-of-sight for air-to-ground radio propagation in urban environments. *Proceedings of IEEE Globecom 2006*, 2006. p. 1-5.
[31] Goldsmith A. *Wireless communications*. Cambridge university press. 2005.
[32] Khuwaja AA, Zheng G, Feng W, Chen Y. Coverage Area Performance for Multiple Interfering UAVs. *Proceedings of 2019 IEEE Global Communications Conference*. *IEEE GLOBECOM 2019*. 2019. p. 1-6.
[33] Colpaert A, Vinogradov E, Pollin S. Aerial coverage analysis of cellular systems at LTE and mmWave frequencies using 3D city models. *Sensors*. 2018. 18(12): 4311.
[34] Kennedy J, Eberhart R. Particle swarm optimization. *Proceedings of IEEE International Conference on Neural Networks*, IEEE ICNN'95. 1995. 4: 1942-1948.
[35] Lee CY, Kang HG. Cell planning with capacity expansion in mobile communications: A tabu search approach. *IEEE Transactions on Vehicular Technology*. 2000. 49(5): 1678-1691.
[36] Mitchell M. *An introduction to genetic algorithms*. MIT Press. 1998.
[37] Lala V, Ndreveloarisoa AF, Wang Desheng; R. Feno Heriniaina; Nour Mohammad Murad; Glauco Fontgalland. Channel Modelling for UAV Air-to-Ground Communication. *2024 5th International Conference on Emerging Trends in Electrical, Electronic and Communications Engineering* (*ELECOM*), *Balaclava*, *Mauritius*, 2024, p. 1-5.
[38] He Y, Hou T, Wang M. A new method for unmanned aerial vehicle path planning in complex environments. *Sci Rep*. 2024; 14(9257): 1-12.
[39] Lin X, Wang C, Wang K, Li M, Yu X. Trajectory planning for unmanned aerial vehicles in complicated urban environments: A control network approach. *Transportation Research Part C: Emerging Technologies*, 2021; 128(103120): 1-22.
[40] Moradi Sizkouhi AM, Majid Esmailifar S, Aghaei M, Vidal de Oliveira AK, Rüther R. Autonomous Path Planning by Unmanned Aerial Vehicle (UAV) for Precise Monitoring of Large-Scale PV plants. *2019 IEEE 46th Photovoltaic Specialists Conference* (*PVSC*), *Chicago*, *IL*, *USA*, 2019, p. 1398-1402
[41] Sharma V, Srinivasan K, Chao H-C, Hua K-L, Cheng W-H. Intelligent deployment of UAVs in 5G heterogeneous communication environment for improved coverage. *Journal of Network and Computer Applications*, 2017; 85(2017): 94-105.
[42] Jawhar I, Mohamed N, Al-Jaroodi J, Agrawal DP, Zhang S. Communication and networking of UAV-based systems: Classification and associated architectures. *Journal of Network and Computer Applications*, 2017; 84(2017): 93-108.
[43] Tanveer J, Haider A, Ali R, Kim A. An Overview of Reinforcement Learning Algorithms for Handover Management in 5G Ultra-Dense Small Cell Networks. *Applied Sciences*, 2022; 12(1): 426, 1-25.
[44] He L, Nabil A, Song B. Explainable Deep Reinforcement Learning for UAV Autonomous Navigation. *Arxiv Preprint PDF paper*, 2021, https://arxiv.org/abs/2009.14551: 1-21.
[45] Taufique A, Jaber M, Imran A, Dawy Z, Yacoub E. Planning Wireless Cellular Networks of Future: Outlook, Challenges and Opportunities. *IEEE Access*, 2017; 5: 4821-4845.

[46] Hayal, M.R., Elsayed, E.E., Kakati, D. et al. Modeling and investigation on the performance enhancement of hovering UAV-based FSO relay optical wireless communication systems under pointing errors and atmospheric turbulence effects. *Opt Quant Electron* 55, 625 (2023).
[47] Elsayed, E.E. Investigations on OFDM UAV-based free-space optical transmission system with scintillation mitigation for optical wireless communication-to-ground links in atmospheric turbulence. *Opt Quant Electron* 56, 837 (2024).
[48] Ravelo B. Distributed NGD active circuit for RF-microwave communication. *AEU-International Journal of Electronics and Communications*. 2014. 68(4): 282-290.
[49] Ravelo B, Fontgalland G, Silva HS, Nebhen J, Rahajandraibe W, Guerin M, Chan G, Wan F. Original Application of Stop-Band Negative Group Delay Microwave Passive Circuit for Two-Step Stair Phase Shifter Designing. IEEE Access. 2021. 10: 1493-1508.
[50] Lalléchère S, Rajaoarisoa L, Clavier L, Galan RS, Ravelo B. Bandpass NGD function design for 5G microwave signal delay synchronization application. Comptes Rendus Physique. 2021. 22(S1): 53-71.
[51] Ravelo B, Lalléchère S, Thakur A, Saini A, Thakur P. Theory and circuit modeling of baseband and modulated signal delay compensations with low-and band-pass NGD effects. *AEU-International Journal of Electronics and Communications*. 2016. 70(9): 1122-1127.
[52] Ravelo B, Rahajandraibe W, Gan Y, Wan F, Murad NM, Douyère A. Reconstruction technique of distorted sensor signals with low-pass NGD function. *IEEE Access*. 2020. (8): 92182-92195.